

## Resveratrol Targeting of Carcinogen-Induced Brain Endothelial Cell Inflammation Biomarkers MMP-9 and COX-2 is Sirt1-Independent

Borhane Annabi<sup>1</sup>, Simon Lord-Dufour<sup>2</sup>, Amélie Vézina<sup>1</sup> and Richard Béliveau<sup>2</sup>

<sup>1</sup>Laboratoire d'Oncologie Moléculaire, <sup>2</sup>Laboratoire de Médecine Moléculaire, Centre de Recherche BioMED, Université du Québec à Montréal, Quebec, Canada. Corresponding author email: [annabi.borhane@uqam.ca](mailto:annabi.borhane@uqam.ca)

**Abstract:** The occurrence of a functional relationship between the release of metalloproteinases (MMPs) and the expression of cyclooxygenase (COX)-2, two inducible pro-inflammatory biomarkers with important pro-angiogenic effects, has recently been inferred. While brain endothelial cells play an essential role as structural and functional components of the blood-brain barrier (BBB), increased BBB breakdown is thought to be linked to neuroinflammation. Chemopreventive mechanisms targeting both MMPs and COX-2 however remain poorly investigated. In this study, we evaluated the pharmacological targeting of Sirt1 by the diet-derived and anti-inflammatory polyphenol resveratrol. Total RNA, cell lysates, and conditioned culture media from human brain microvascular endothelial cells (HBMEC) were analyzed using qRT-PCR, immunoblotting, and zymography respectively. Tissue scan microarray analysis of grade I–IV brain tumours cDNA revealed increased gene expression of Sirt-1 from grade I–III but surprisingly not in grade IV brain tumours. HBMEC were treated with a combination of resveratrol and phorbol 12-myristate 13-acetate (PMA), a carcinogen known to increase MMP-9 and COX-2 through NF- $\kappa$ B. We found that resveratrol efficiently reversed the PMA-induced MMP-9 secretion and COX-2 expression. Gene silencing of Sirt1, a critical modulator of angiogenesis and putative target of resveratrol, did not lead to significant reversal of MMP-9 and COX-2 inhibition. Decreased resveratrol inhibitory potential of carcinogen-induced I $\kappa$ B phosphorylation in siSirt1-transfected HBMEC was however observed. Our results suggest that resveratrol may prevent BBB disruption during neuroinflammation by inhibiting MMP-9 and COX-2 and act as a pharmacological NF- $\kappa$ B signal transduction inhibitor independent of Sirt1.

**Keywords:** angiogenesis, inflammation, resveratrol, brain endothelial cells, MMP-9, COX-2, Sirt1

*Drug Target Insights* 2012:6 1–11

doi: [10.4137/DTI.S9442](https://doi.org/10.4137/DTI.S9442)

This article is available from <http://www.la-press.com>.

© the author(s), publisher and licensee Libertas Academica Ltd.

This is an open access article. Unrestricted non-commercial use is permitted provided the original work is properly cited.



## Introduction

Tumour-associated angiogenesis, a fundamental process in tumour growth and metastasis, consists of recruiting EC toward an angiogenic stimulus.<sup>1</sup> The cells subsequently proliferate and differentiate to form endothelial tubes and capillary-like structures in order to deliver nutrients and oxygen to the tumour and to remove the products of its metabolism. In recent years, several pathways have, in addition to stimulation of tumor angiogenesis, been suggested to contribute to the cell metabolic adaptations required for carcinogenesis, which include decreased tumoural apoptosis, increased invasion and metastasis, immune suppression and tumour-associated inflammation.<sup>2,3</sup> An interesting link between overexpression of pro-inflammatory markers such as matrix metalloproteinase-9 (MMP-9) and cyclooxygenase (COX)-2, and tumour angiogenesis was recently described as one such metabolic adaptive phenotype.<sup>4-6</sup> While flavonoids and related polyphenolic compounds, such as resveratrol, have demonstrated significant antiinflammatory activity, predominantly, through the inhibition of NF- $\kappa$ B signaling,<sup>7</sup> their potential therapeutic application upon the cerebral vascular compartment in neuroinflammation still remains poorly documented.

While human brain microvascular endothelial cells (HBMEC) play an essential role as structural and functional components of the blood-brain barrier (BBB), its disruption by MMP-9 is believed to favor tumor invasion.<sup>8,9</sup> Recent studies in fact delineated a unique brain endothelial phenotype in which MMP-9 secretion by HBMEC was increased upon treatment with the tumor-promoting agent phorbol 12-myristate 13-acetate (PMA).<sup>10,11</sup> Inhibition of MMP-9 secretion was demonstrated to reduce both in vitro invasion and angiogenesis in human microvascular EC.<sup>12</sup> Among the signalling pathways involved, NF- $\kappa$ B signalling was the one that enabled the joint control of both MMP-9 and COX-2 inflammation marker expression.<sup>13,14</sup>

Recent studies point to Sirt1, the most widely investigated and best known sirtuin, as a key regulator of vascular endothelial homeostasis controlling angiogenesis, vascular tone and endothelial dysfunction.<sup>15</sup> Sirtuins are a family of conserved proteins with deacetylase and ADP-ribosyltransferase activity encoded in humans by seven genes (Sirt1-7).<sup>16</sup>

In cancer cells, conflicting reports regarding the expression of Sirt1 show either up-regulation<sup>17,18</sup> or downregulation<sup>19</sup> of Sirt1. Sirt1 may thus play a critical role in tumor progression, and drug resistance. While Sirt1 inhibitors have shown promising anticancer effects in animal models of cancer, its implication in a brain EC model has yet to be documented. More importantly, the expression of Sirt1 in the brain EC compartment as well as impact of its pharmacological targeting is still unknown. Given that Sirt1-independent mechanisms were recently reported in the action of resveratrol,<sup>20</sup> this current study therefore focuses on resveratrol as a potential signal transduction inhibitor of carcinogen-mediated induction of the NF- $\kappa$ B pathway in a human brain EC model and questions the involvement of Sirt1.

## Materials and Methods

### Reagents and cell culture

Bovine serum albumin (BSA) was purchased from MyClone Laboratories (Logan, UT). Electrophoresis reagents were purchased from Bio-Rad (Mississauga, ON). The enhanced chemiluminescence (ECL) reagents were from Perkin Elmer (Waltham, MA). Micro bicinchoninic acid protein assay reagents were from Pierce (Rockford, IL). The polyclonal antibodies against I $\kappa$ B and phospho-I $\kappa$ B were purchased from Cell Signaling (Danvers, MA). The monoclonal antibody against GAPDH was from Advanced Immunochemical Inc. (Long Beach, CA). Horseradish peroxidase-conjugated donkey anti-rabbit and anti-mouse IgG secondary antibodies were from Jackson ImmunoResearch Laboratories (West Grove, PA). Sodium dodecylsulfate (SDS) and all other reagents were from Sigma-Aldrich Canada. Human brain microvascular endothelial cells (HBMEC) were characterized and generously provided by Dr. Kwang Sik Kim of the Johns Hopkins University School of Medicine (Baltimore, MD).<sup>21,22</sup> Cells were cultured at 37 °C under a humidified atmosphere containing 5% CO<sub>2</sub>. All experiments were performed using passages 3 to 28.

### Gelatin zymography and immunoblotting procedures

Proteins from control and treated cells were separated by SDS-PAGE, and electrotransferred to polyvinylidene difluoride membranes as previously described.<sup>21</sup> Gelatin zymography was used to assess the extent of



proMMP-9 activity as previously described.<sup>23</sup> Briefly, an aliquot (20  $\mu$ L) of the culture medium was subjected to SDS-PAGE in a gel containing 0.1 mg/mL gelatin. The gels were then incubated in 2.5% Triton X-100 and rinsed in nanopure distilled H<sub>2</sub>O. Gels were further incubated at 37 °C for 20 hrs in 20 mM NaCl, 5 mM CaCl<sub>2</sub>, 0.02% Brij-35, 50 mM Tris-HCl buffer, pH 7.6, then stained with 0.1% Coomassie Brilliant blue R-250 and destained in 10% acetic acid, 30% methanol in H<sub>2</sub>O. Gelatinolytic activity was detected as unstained bands on a blue background.

### Total RNA isolation, cDNA synthesis and real-time quantitative RT-PCR

Total RNA was extracted from cell monolayers using TriZol reagent (Life Technologies, Gaithersburg, MD). For cDNA synthesis, 2  $\mu$ g of total RNA were reverse-transcribed using a high capacity cDNA reverse transcription kit (Applied Biosystems, Foster City, CA). cDNA was stored at -80 °C prior to PCR. Gene expression was quantified by real-time quantitative PCR using iQ SYBR Green Supermix (Bio-Rad, Hercules, CA). DNA amplification was carried out using an Icyler iQ5 (Bio-Rad, Hercules, CA) and product detection was performed by measuring binding of the fluorescent dye SYBR Green I to double-stranded DNA. The QuantiTect primer sets were provided by Qiagen (Valencia, CA): MMP-9 (QT00040040), COX-2 (QT00040586),  $\beta$ -Actin (QT01136772). GAPDH primer sets were synthesized by Biocorp (Dollard-des-Ormeaux, QC) with the following sequences: forward CCATCACCATCTTCCAGGAG and reverse CCTGCTTACCACCTTCTTG. The relative quantities of target gene mRNA compared against two internal controls, GAPDH and  $\beta$ -Actin mRNA, were measured by following a  $\Delta C_T$  method employing an amplification plot (fluorescence signal vs. cycle number). The difference ( $\Delta C_T$ ) between the mean values in the triplicate samples of target gene and those of GAPDH and  $\beta$ -actin mRNAs were calculated by iQ5 Optical System Software version 2.0 (Bio-Rad, Hercules, CA) and the relative quantified value (RQV) was expressed as  $2^{-\Delta C_T}$ .

### TissueScan cDNA arrays of grade I-IV brain tumour tissues

TissueScan™ cancer and normal tissue cDNA arrays were purchased from OriGene (Rockville, MD),

covered 43 clinical samples of the brain cancer four stages and normal tissues, and were used to analyze differential Sirt1 gene expression according to the manufacturer's recommendation. Tissue cDNAs of each array are synthesized from high quality total RNAs of pathologist-verified tissues, normalized and validated with  $\beta$ -actin in two sequential qPCR analyses, and provided with clinical information for 2 normal brain, 18 WHO grade I, 11 WHO grade II, 10 WHO grade III, and 2 WHO grade IV brain tumours.

### Transfection method and RNA interference

Cells were transiently transfected with 20 nM siRNA (Qiagen) against Sirt1 (Hs\_SIRT1\_1 FlexiTube siRNA, SI00098434) or scrambled sequences (AllStar Negative Control siRNA, 1027281) using Lipofectamine 2000 (Invitrogen, ON). Specific gene knockdown was evaluated by qRT-PCR as described above. Small interfering RNA and mismatch siRNA were synthesized by Qiagen (Valencia, CA) and annealed to form duplexes.

### Statistical data analysis

Data statistical significance ( $P$  values <0.05) was assessed using Student's unpaired  $t$ -test from three or more independent experiments.

## Results

### Sirt1 gene expression profiling in grade I-IV brain tumour tissues

Fourty-eight clinical tissue samples were first analyzed for Sirt1 gene expression profile using TissueScan™ cancer and normal tissue cDNA arrays (OriGene, Rockville, MD) from 43 clinical samples covering brain cancer four stages and normal tissues as described in the methods section. We found that Sirt1 gene expression levels increased from grade I to grade III brain tumour tissues (Fig. 1, black bars), but not in grade IV as compared to normal brain tissue (Fig. 1, white bars). This suggests that discrepancy found in the literature regarding Sirt1 expression in tissue samples may be explained by the invasive stage status of a given tumour. Given that tumour samples are composed of a heterogeneous cell composition including

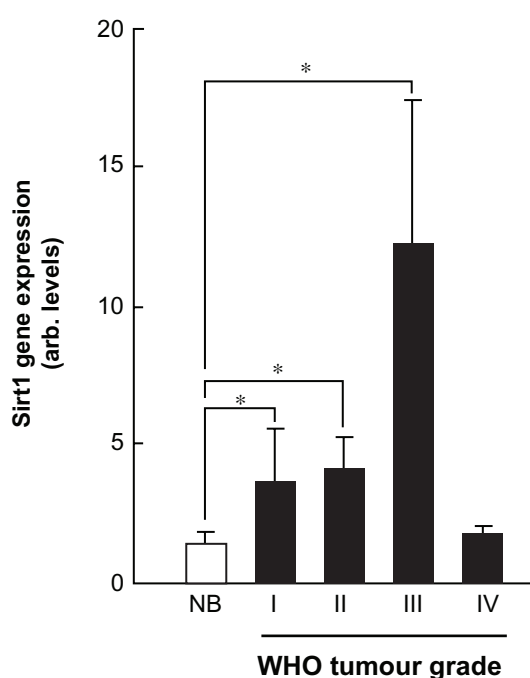


**Figure 1.** Sirt1 gene expression profiling in grade I-IV brain tumour tissues. TissueScan™ cancer and normal tissue cDNA arrays from 43 clinical samples covering brain cancer four stages and normal brain tissues were used to analyze differential Sirt1 gene expression. Tissue cDNAs of each array are synthesized from high quality total RNAs of pathologist-verified tissues, normalized and validated with  $\beta$ -actin and provided with clinical information for 2 normal brain, 18 WHO grade I, 11 WHO grade II, 10 WHO grade III, and 2 WHO grade IV brain tumours.

**Abbreviation:** NB, normal brain tissue.

cancer, inflammatory, as well as endothelial cells, we decided to focus our study on the Sirt1 contribution within a carcinogen-treated brain-associated endothelial cell compartment.

### Resveratrol dose-dependent inhibition of carcinogen-induced COX-2 gene and protein expression

Various molecular mechanisms mediate inflammatory processes and angiogenesis, one of which is reflected by increased expression of the inflammatory biomarker COX-2.<sup>7</sup> In order to investigate the effect of resveratrol on HBMEC-associated inflammation, we tested the effects of resveratrol on PMA-induced cell signaling in HBMEC by Western blotting. Cells were therefore treated with 1  $\mu$ M of PMA in the presence of increasing concentrations of resveratrol for 18h and COX-2 expression was evaluated in cell lysates by Western Blotting (Fig. 2A). While 100  $\mu$ M resveratrol was without effect on COX-2 basal expression, it significantly inhibited PMA-induced COX-2

protein expression ( $IC_{50}$  6.1  $\pm$  2.2  $\mu$ M, Fig. 2B) and gene (Fig. 2C) expression.

### Resveratrol inhibition of carcinogen-induced MMP-9 gene expression and protein secretion

Among the secreted enzymes involved in ECM degradation, matrix metalloproteinases (MMP) are well-documented as being involved in EC migration and tubulogenesis.<sup>10,24</sup> MMP-9, an enzyme involved in the degradation of the extracellular matrix (ECM), is secreted by a variety of cells and its presence was shown to be increased upon carcinogen promoting agents such as the phorbol ester PMA.<sup>25-27</sup> HBMEC were first treated for 18 h with PMA. Gelatin zymography was then used to measure proMMP-9 levels, which were significantly increased upon PMA treatment in comparison to vehicle-treated cells (Fig. 3A). Addition of increasing concentrations of resveratrol to PMA-treated cells resulted in a dose-dependent inhibition of MMP-9 activity ( $IC_{50}$  9.1  $\pm$  0.8  $\mu$ M, Fig. 3B and C). It was found that PMA also increased MMP-9 gene expression while the presence of resveratrol inhibited this increase suggesting transcriptional regulation of the MMP-9 gene (Fig. 3D).

### Carcinogen-induced I $\kappa$ B phosphorylation is inhibited by resveratrol

Among MMP-9 expression regulators, the nuclear factor-kappaB (NF- $\kappa$ B) signalling pathway has been demonstrated to link cancer to inflammatory diseases.<sup>28</sup> We therefore assessed whether this signalling was activated upon PMA treatment and whether it was reflected in I $\kappa$ B degradation. HBMEC were serum-starved then treated with 1  $\mu$ M PMA for up to 30 minutes, lysates were isolated and I $\kappa$ B phosphorylation was assessed through Western Blotting (Fig. 4A, upper panel). PMA signalling led to the phosphorylation of I $\kappa$ B peaking at 15 minutes.<sup>29</sup> Resveratrol effect on PMA-mediated phosphorylation of I $\kappa$ B was next assessed in order to demonstrate whether this mechanism contributes to the anti-COX-2 inhibitory activities of resveratrol. Preincubation with 30  $\mu$ M resveratrol followed by a 30 min PMA treatment led to diminished I $\kappa$ B phosphorylation as demonstrated by the decreased ratios of phosphorylated I $\kappa$ B over GAPDH expression (Fig. 4B).

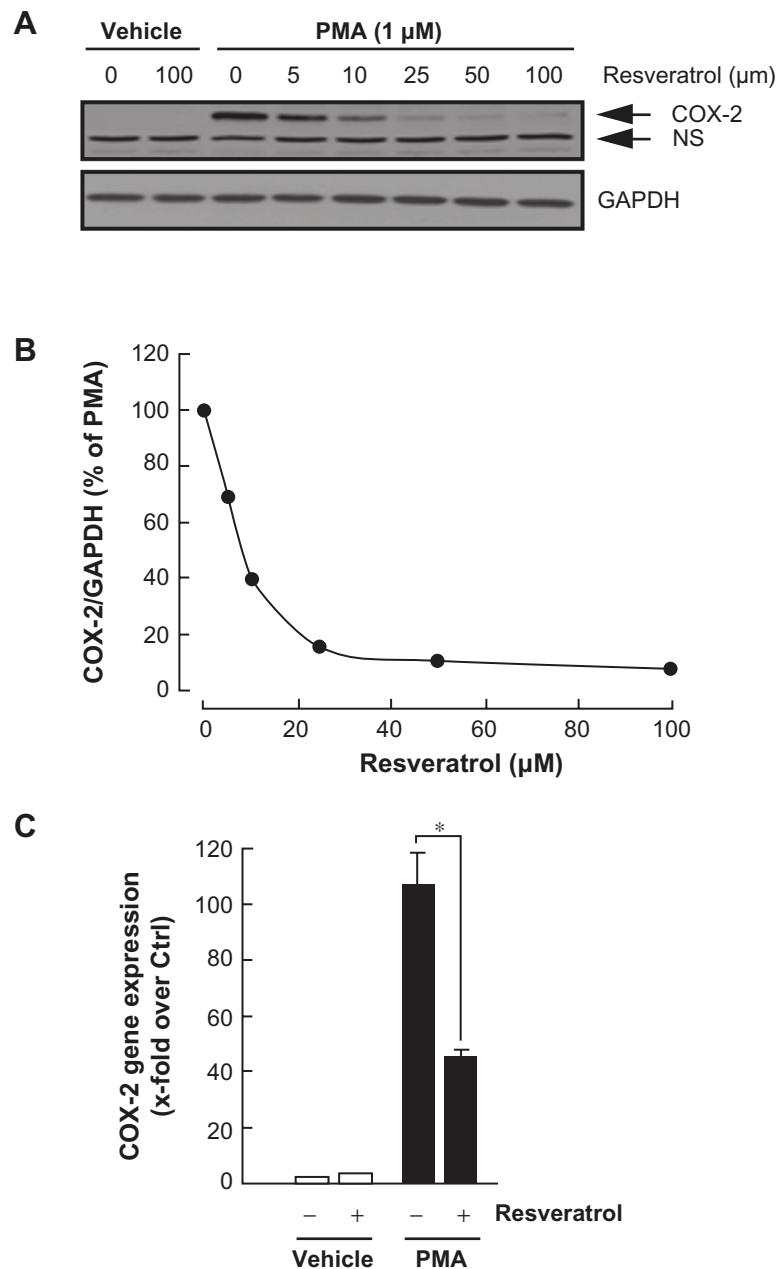


**Figure 2.** Resveratrol dose-dependent inhibition of carcinogen-induced COX-2 protein and gene expression. **(A)** HBMEC were serum-starved in the presence of various concentrations of resveratrol and in combination with vehicle or 1  $\mu$ M PMA for 18 hours. Lysates were isolated, electrophoresed via SDS-PAGE, and immunodetection of COX-2 and GAPDH performed as described in the Methods section (NS, non specific immunoreactivity). **(B)** Scanning densitometry of COX-2 expression was only performed in PMA-treated cells since no COX-2 was detectable in vehicle-treated HBMEC. Densitometric data of a representative blot is shown out of three independent experiments. **(C)** Total RNA isolation, RT-PCR, and qPCR were performed as described in the Methods section to assess COX-2 gene expression in the above-described conditions. (PMA = 1  $\mu$ M; Resveratrol = 30  $\mu$ M).

**Notes:** Data are representative of three independent qPCR experiments. Probability values of less than 0.05 were considered significant, and an asterisk (\*) identifies such significance to the respective PMA treatment.

## Sirt1 contributes to the resveratrol inhibitory effect of PMA-induced I $\kappa$ B phosphorylation

Sirt1 is, among the sirtuins family, documented to be targeted by resveratrol. In order to assess the

contribution of Sirt1 in the resveratrol inhibition of NF- $\kappa$ B, HBMEC were next transiently transfected with a scrambled siRNA sequence (Mock) or an siRNA designed to downregulate Sirt1 (siSirt1) gene expression. Preincubation with 30  $\mu$ M resveratrol followed by a 30 min PMA treatment was performed

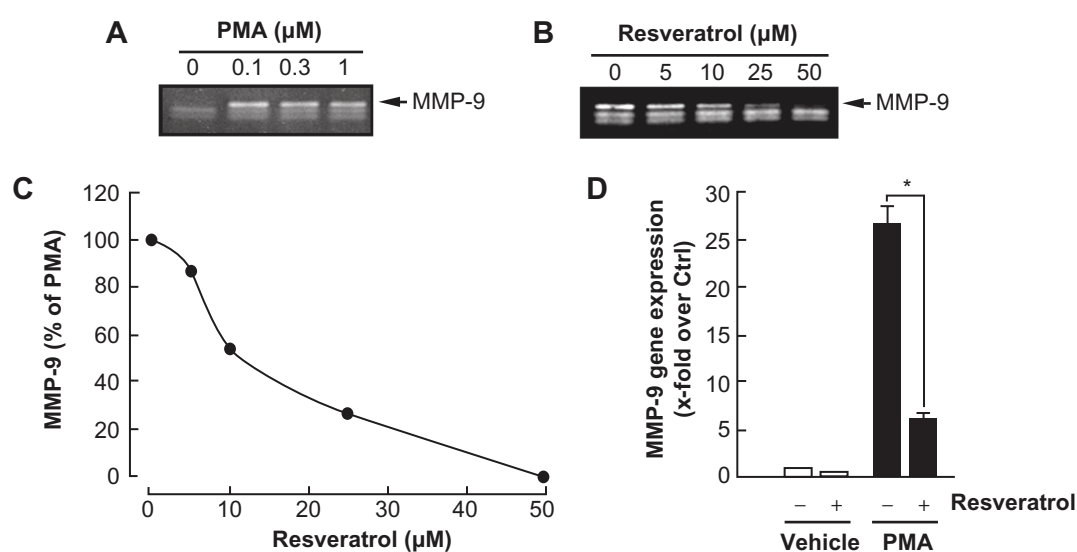


**Figure 3.** Resveratrol inhibition of carcinogen-induced MMP-9 gene expression and protein secretion. HBMEC were serum-starved in the presence of (A) various PMA concentrations for 18 hours, or (B) a combination of 1  $\mu$ M PMA with increasing resveratrol concentrations. Conditioned media were then harvested and gelatin zymography was performed in order to detect PMA-induced proMMP-9 and hydrolytic activity as described in the Methods section. (C) Scanning densitometry was used to quantify the extent of proMMP-9 gelatinolytic activity in the combined PMA and resveratrol treatments. Data shown is representative of two independent experiments. (D) Total RNA isolation and qRT-PCR were performed as described in the Methods section to assess MMP-9 gene expression in the above-described conditions. (PMA = 1  $\mu$ M; Resveratrol = 30  $\mu$ M).

**Notes:** Data are representative of three independent qPCR experiments. Probability values of less than 0.05 were considered significant, and an asterisk (\*) identifies such significance to the respective PMA treatment.

in Mock and in siSirt1-transfected cells. Lysates were isolated, and GAPDH or I $\kappa$ B phosphorylation assessed through Western Blotting (Fig. 5A, upper panel). While ~90% inhibition in Sirt1 gene expression was observed in siSirt1-transfected cells (Fig. 5B), we found that resveratrol inhibitory potential was significantly diminished in those cells which had Sirt1 expression silenced (Fig. 5C, closed circles) in comparison to Mock-transfected cells (Fig. 5C, open circles). PMA treatment by itself did not affect Sirt1 gene expression (not shown). This suggests that Sirt1 is indeed important in the inhibitory potential of resveratrol against PMA-mediated NF- $\kappa$ B signaling pathway.

### Sirt1-independent inhibition by resveratrol of PMA-induced COX-2 expression and of PMA-induced MMP-9 secretion

Whether Sirt1 serves as an intermediate in the resveratrol inhibitory potential was next investigated on PMA-treated cells for COX-2 and MMP-9 expression. As described above, serum-starved mock and siSirt1-transfected HBMEC were treated with PMA, resveratrol or a combination of both agents. While resveratrol efficiently inhibited

both PMA-induced COX-2 (Fig. 6A) and MMP-9 (Fig. 6B), silencing of Sirt1 did not lead to any reversal of effect as resveratrol still efficiently inhibited COX-2 and MMP-9. This suggests that resveratrol inhibition of PMA-induced COX-2 and MMP-9 is a Sirt1 independent event.

### Discussion

The adaptive mechanisms responsible for EC metabolic adaptation and survival under pro-carcinogenic stimulation, or as encountered within a tumour microenvironment, still remain poorly documented. While interest has been manifested towards cancer therapies that jointly target EC angiogenic and inflammatory phenotypes, the design, synthesis and evaluation of flavonoid derivatives that target neurodegenerative disorders have accordingly paved the road to strategies leading to decreased extracellular matrix (ECM) degradation and inflammation processes.<sup>30</sup> The objectives of this current study were first to trigger in vitro pro-carcinogenic stimulation of a brain microvascular EC model using PMA in combination with resveratrol, and assess impact on inflammation biomarkers MMP-9 and COX-2 expression. Secondly, given that resveratrol is a well documented pharmacological agonist of Sirt1,

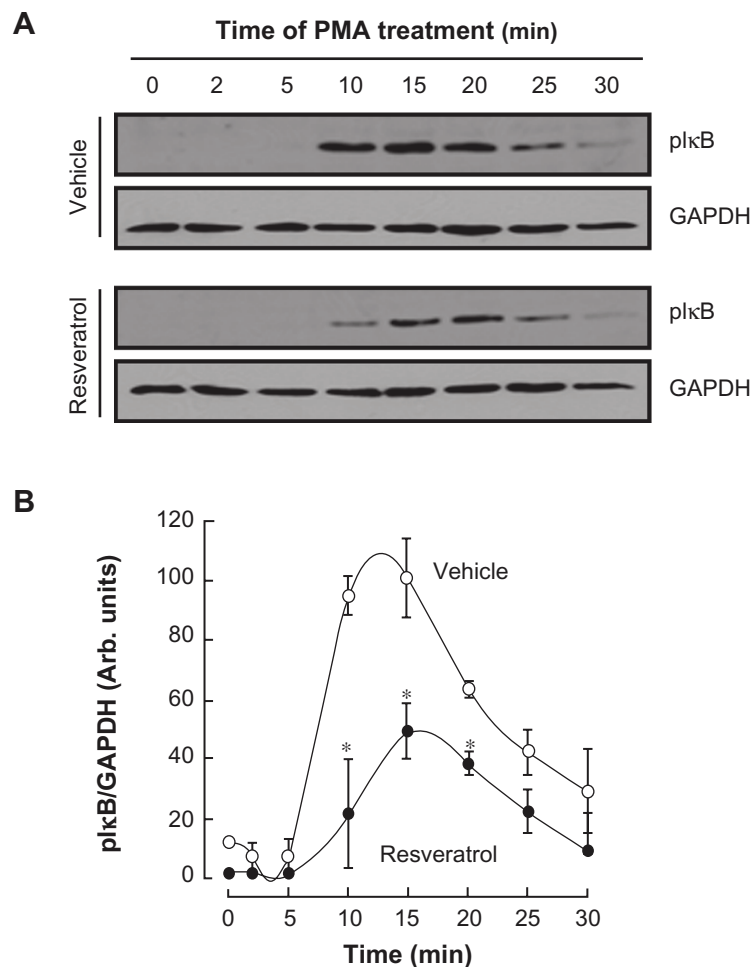


**Figure 4.** Carcinogen-induced IκB phosphorylation is inhibited by resveratrol. **(A)** HBMEC were serum-starved for 30 minutes in the presence or not of 30 μM resveratrol, then treated with 1 μM PMA for the indicated time. Lysates were isolated, electrophoresed via SDS-PAGE and immunodetection of phosphorylated IκB (P-IκB) and GAPDH proteins was performed as described in the Methods section. **(B)** Quantification was performed by scanning densitometry of the autoradiograms.

**Notes:** Data were expressed as the percent of basal phospho-IκB/GAPDH ratios in vehicle (open circles) and resveratrol pre-treated cells (closed circles). Densitometric data of a representative blot out of three is shown.

but that conflicting data regarding Sirt1 expression in glioblastoma has been reported,<sup>17–19</sup> we specifically explored its contribution to the resveratrol anti-PMA pharmacological properties.

Our first objective was confirmed by the increases in inflammatory biomarkers MMP-9 and COX-2 expression upon carcinogenic stimulation in HBMEC. As such, the calculated IC<sub>50</sub> concentrations of resveratrol inhibitory effects extracted from our in vitro model closely approximate those actual concentrations assessed in the plasma ranging between 1.2–2.6 μM.<sup>31,32</sup> Both biomarkers expression was inhibited by resveratrol and this required inhibition of the NF-κB signaling pathway as validated by reduced IκB phosphorylation. Inhibition of NF-κB (p65 subunit) translocation to the nucleus

by resveratrol is a mechanism that has already been inferred in an experimental hepatocarcinogenesis model.<sup>33</sup> Our data thus indirectly support this nuclear translocation effect since IκB phosphorylation, which ultimately releases p65 and p50 in order to allow nuclear translocation, was found inhibited by resveratrol in our model (Fig. 4B). Although not the scope of this study, ChIP assays may further help address NF-κB capacity to bind COX-2 and MMP-9 promoter regions.

Given that the involvement of Sirt1 still remains undefined, at least within the carcinogenic context we report herein, our second objective was evaluated and confirmed a Sirt1-independent, but efficient, targeting by resveratrol of the PMA-induced NF-κB signaling pathway that ultimately leads to reduced

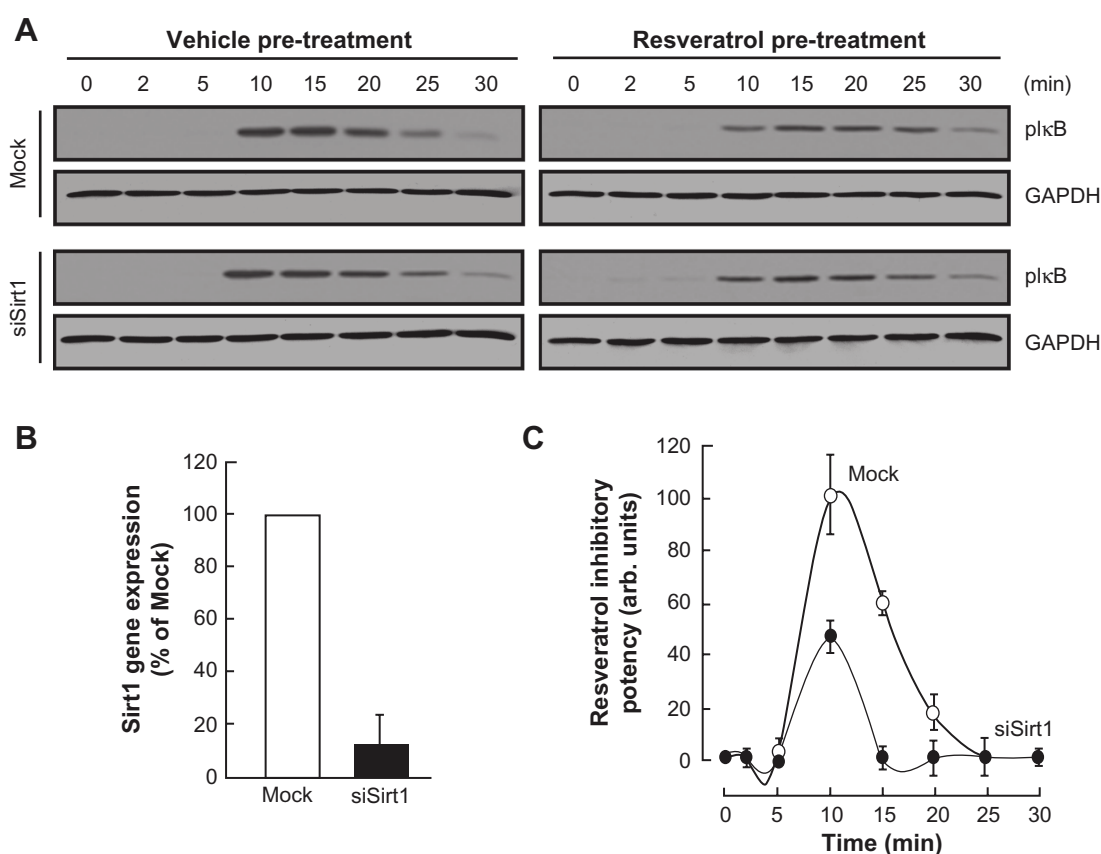


**Figure 5.** Sirt1 contributes to the resveratrol inhibitory effect of PMA-induced I $\kappa$ B phosphorylation. HBMEC were transiently transfected with a scrambled siRNA sequence (Mock) or a siRNA designed to downregulate Sirt1 (siSirt1) as described in the Methods section. (A) Mock and siSirt1-transfected HBMEC were then serum-starved for 30 minutes in the presence or not of 50  $\mu$ M resveratrol, then treated with 1  $\mu$ M PMA for the indicated time. Lysates were isolated, electrophoresed via SDS-PAGE and immunodetection of phosphorylated I $\kappa$ B (P-I $\kappa$ B) and GAPDH proteins was performed as described in the Methods section. (B) Total RNA isolation, RT-PCR, and qPCR were performed as described in the Methods section to assess Sirt1 gene expression in the Mock and siSirt1-transfected HBMEC. (C) Quantification was performed by scanning densitometry of the autoradiograms obtained in (A).

**Notes:** Data were expressed as the percent of basal phospho-I $\kappa$ B/GAPDH ratios in vehicle (open circles) and resveratrol pre-treated cells (closed circles). Densitometric data of a representative blot out of three is shown.

MMP-9 and COX-2 expression. Our current data do not support Sirt1 requirements in our brain EC model suggesting that cell specificity may dictate resveratrol efficacy in inhibiting MMP-9 in neuroinflammation or brain tumor angiogenesis. In accordance with our current study, the presence or absence of Sirt1, as assessed through the use of Sirt1-null animals, had no effect on incidence and tumor load induced by a two-stage carcinogenesis protocol.<sup>42</sup> In fact, only part of the chemopreventive effect of resveratrol was attributed to Sirt1.<sup>34</sup> Moreover, while most biological effects of sirtuins have so far been attributed to their enzymatic activity, opposing effects of sirtuins on neuronal survival have also been reported suggestive of Sirt1-mediated neuroprotection independent of deacetylase activity.<sup>35</sup> Although resveratrol is a potent pharmacological agonist of Sirt1,<sup>36</sup> and expected

to induce deacetylation of known Sirt1 substrates such as NF- $\kappa$ B, PGC-1 $\alpha$ , and p53,<sup>37,38</sup> one may now have to consider alternate mechanisms of resveratrol to those mediated through Sirt1. Among those mechanisms, several flavonoids have been reported to interfere with the inducible nitric-oxide synthase activity, as well as of both the COX and 5-lipoxygenase pathways.<sup>39,40</sup> Interestingly, Sirt1 is a putative suppressive regulator found in the MMP-9 gene promoter,<sup>41</sup> and activation of Sirt1 by resveratrol was found to be required for inhibition of PMA-induced MMP-9 expression.<sup>42,43</sup>

Generalized interpretation, in part due to the occurrence of multiple in vitro cell culture models, has put forward large number of mechanisms of action attributed to flavonoids commonly found in fruits, vegetables, wine, or tea as their metabolites also can act

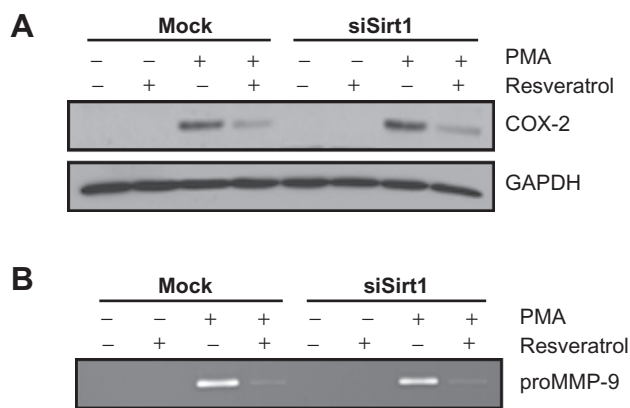


**Figure 6.** Sirt1-independent inhibition by resveratrol of PMA-induced COX-2 expression and of PMA-induced MMP-9 secretion. Mock or siSirt1-transfected HBMEC were serum-starved in the presence of 1  $\mu$ M PMA, 30  $\mu$ M resveratrol, or a combination of both agents for 18 hours. **(A)** Lysates were isolated, electrophoresed via SDS-PAGE, and immunodetection of COX-2 and GAPDH performed as described in the Methods section. **(B)** Conditioned media were also harvested and gelatin zymography was performed in order to detect PMA-induced proMMP-9 and hydrolytic activity as described in the Methods section.

as potent antioxidants and free radical scavengers.<sup>21,44</sup> Whether the inhibitory effects observed *in vitro* are due to resveratrol metabolites has therefore to be promptly considered and carefully addressed. As such, oral bioavailability of resveratrol has been reported to be low because it is rapidly metabolized in intestines and liver into conjugated forms such as glucuronate and sulfonate.<sup>45</sup> In mammals, less than 5% of the oral dose is being observed as free resveratrol in blood plasma.<sup>45–47</sup> The most abundant resveratrol metabolites being trans-resveratrol-3-O-glucuronide and trans-resveratrol-3-sulfate,<sup>48</sup> the impact of glucuronides and of these sulfate conjugates will also ultimately need further study.

In summary, the present study has confirmed resveratrol as a signal transduction inhibitor against carcinogen-mediated induction of COX-2 and MMP-9. Moreover, evidence that the NF- $\kappa$ B pathway may be inhibited through the targeting of I $\kappa$ K phosphorylation capacity that ultimately may reduce both the acquisition of a pro-inflammatory phenotype, as reflected by decreased COX-2 expression, and the acquisition of pro-angiogenic phenotype, as reflected by a decrease in MMP-9. Our results further discriminate the role of Sirt1 in the anti-PMA action of resveratrol suggesting alternative intracellular targeting. Whether other sirtuin members are involved remains to be investigated. BBB disruption

during neuroinflammation may, in light of our results, be pharmacologically reduced by a specific class of flavonoids acting as NF- $\kappa$ B signal transduction inhibitors.

## List of Abbreviations

BBB, blood-brain barrier; COX, cyclooxygenase; EC, endothelial cells; ER, endoplasmic reticulum; MMP-9, matrix metalloproteinase-9; NF- $\kappa$ B, nuclear factor-kappa B; PMA, phorbol 12-myristate 13-acetate.

## Authors' Contributions

BA has conceived, designed, analyzed and interpreted the data of this study. SLD has acquired, analyzed, and was involved in drafting the manuscript. AV has acquired and analyzed the data. RB has conceived, designed, supported financially this study, and was involved in drafting the manuscript. All authors read and approved the final version of this manuscript.

## Competing Interests

BA holds a Canada Research Chair in Molecular and Metabolic Oncology from the Canadian Institutes of Health Research (CIHR). RB holds an Institutional UQAM Research Chair in Cancer Prevention and Treatment.

## Funding

This study was funded by grants from the Natural Sciences and Engineering Research Council of Canada (NSERC) to RB.

## Disclosures and Ethics

As a requirement of publication author(s) have provided to the publisher signed confirmation of compliance with legal and ethical obligations including but not limited to the following: authorship and contributorship, conflicts of interest, privacy and confidentiality and (where applicable) protection of human and animal research subjects. The authors have read and confirmed their agreement with the ICMJE authorship and conflict of interest criteria. The authors have also confirmed that this article is unique and not under consideration or published in any other publication, and that they have permission from rights holders to reproduce any copyrighted material. Any disclosures are made in this section.



The external blind peer reviewers report no conflicts of interest.

## References

- Hanahan D, Folkman J. Patterns and emerging mechanisms of the angiogenic switch during tumorigenesis. *Cell*. 1996;86:353–64.
- Rojas A, Figueroa H, Morales E. Fueling inflammation at tumor microenvironment: the role of multiligand/RAGE axis. *Carcinogenesis*. 2010; 31:334–41.
- Hayes A. Cancer, cyclo-oxygenase and nonsteroidal anti-inflammatory drugs—can we combine all three? *Vet Comp Oncol*. 2007;5:1–13.
- Costa C, Soares R, Reis-Filho JS, Leitão D, Amendoeira I, Schmitt FC. Cyclo-oxygenase 2 expression is associated with angiogenesis and lymph node metastasis in human breast cancer. *J Clin Pathol*. 2002;55:429–34.
- Fournier LS, Novikov V, Lucidi V, et al. MR monitoring of cyclooxygenase-2 inhibition of angiogenesis in a human breast cancer model in rats. *Radiology*. 2007;243:105–11.
- Müller-Decker K, Fürstenberger G. The cyclooxygenase-2-mediated prostaglandin signaling is causally related to epithelial carcinogenesis. *Mol Carcinog*. 2007;46:705–10.
- Neerghen VS, Bahorun T, Taylor EW, Jen LS, Aruoma OI. Targeting specific cell signaling transduction pathways by dietary and medicinal phytochemicals in cancer chemoprevention. *Toxicology*. 2010;278:229–41.
- Lakka SS, Gondi CS, Rao JS. Proteases and glioma angiogenesis. *Brain Pathol*. 2005;15:327–41.
- Bonoiu A, Mahajan SD, Ye L, et al. MMP-9 gene silencing by a quantum dot-siRNA nanoplex delivery to maintain the integrity of the blood brain barrier. *Brain Res*. 2009;1282:142–55.
- Annabi B, Rojas-Sutterlin S, Laroche M, Lachambre MP, Moudjian R, Béliveau R. The diet-derived sulforaphane inhibits matrix metalloproteinase-9-activated human brain microvascular endothelial cell migration and tubulogenesis. *Mol Nutr Food Res*. 2008;52:692–700.
- Roomi MW, Monterrey JC, Kalinovsky T, Rath M, Niedzwiecki A. Distinct patterns of matrix metalloproteinase-2 and -9 expression in normal human cell lines. *Oncol Rep*. 2009;21:821–6.
- Jadhav U, Chigurupati S, Lakka SS, Mohanam S. Inhibition of matrix metalloproteinase-9 reduces in vitro invasion and angiogenesis in human microvascular endothelial cells. *Int J Oncol*. 2004;25:1407–14.
- Luqman S, Pezzuto JM. NFkappaB: a promising target for natural products in cancer chemoprevention. *Phytother Res*. 2010;24:949–63.
- Tergaonkar V. NFkappaB pathway: a good signaling paradigm and therapeutic target. *Int J Biochem Cell Biol*. 2006;38:1647–53.
- Potente M, Dimmeler S. Emerging roles of SIRT1 in vascular endothelial homeostasis. *Cell Cycle*. 2008;7:2117–22.
- Schlicker C, Boanca G, Lakshminarasimhan M, Steegborn C. Structure-based development of novel sirtuin inhibitors. *Aging (Albany NY)*. 2011;3: 852–72.
- Liu G, Yuan X, Zeng Z, et al. Analysis of gene expression and chemoresistance of CD133+ cancer stem cells in glioblastoma. *Mol Cancer*. 2006;5:67.
- Chang CJ, Hsu CC, Yung MC, et al. Enhanced radiosensitivity and radiation-induced apoptosis in glioma CD133-positive cells by knockdown of SirT1 expression. *Biochem Biophys Res Commun*. 2009;380:236–42.
- Wang RH, Sengupta K, Li C, et al. Impaired DNA damage response, genome instability, and tumorigenesis in SIRT1 mutant mice. *Cancer Cell*. 2008;14:312–23.
- Centeno-Baez C, Dallaire P, Marette A. Resveratrol inhibition of inducible nitric oxide synthase in skeletal muscle involves AMPK but not SIRT1. *Am J Physiol Endocrinol Metab*. 2011;301:E922–30.
- Tahanian E, Peiro S, Annabi B. Low intracellular ATP levels exacerbate carcinogen-induced inflammatory stress response and inhibit in vitro tubulogenesis in human brain endothelial cells. *J Inflamm Res*. 2011;4:1–10.
- Greiffenberg L, Goebel W, Kim KS, et al. Interaction of *Listeria monocytogenes* with human brain microvascular endothelial cells: InlB-dependent invasion, long-term intracellular growth, and spread from macrophages to endothelial cells. *Infect Immun*. 1998;66:5260–7.
- Sina A, Lord-Dufour S, Annabi B. Cell-based evidence for aminopeptidase N/CD13 inhibitor actinonin targeting of MT1-MMP-mediated proMMP-2 activation. *Cancer Lett*. 2009;279:171–6.
- Abécassis I, Olofsson B, Schmid M, Zalcman G, Karniguian A. RhoA induces MMP-9 expression at CD44 lamellipodial focal complexes and promotes HMEC-1 cell invasion. *Exp Cell Res*. 2003;291:363–76.
- Annabi B, Currie JC, Moghrabi A, Béliveau R. Inhibition of HuR and MMP-9 expression in macrophage-differentiated HL-60 myeloid leukemia cells by green tea polyphenol EGCG. *Leuk Res*. 2007;31:1277–84.
- Tahanian E, Lord-Dufour S, Das A, Khosla C, Roy R, Annabi B. Inhibition of tubulogenesis and of carcinogen-mediated signaling in brain endothelial cells highlight the antiangiogenic properties of a mumbaistatin analog. *Chem Biol Drug Des*. 2010;75:481–8.
- Annabi B, Vaillancourt-Jean E, Weil AG, Béliveau R. Pharmacological targeting of  $\beta$ -adrenergic receptor functions abrogates NF- $\kappa$ B signaling and MMP-9 secretion in medulloblastoma cells. *Onco Targets Ther*. 2010;3: 219–26.
- Dong J, Jimi E, Zeiss C, Hayden MS, Ghosh S. Constitutively active NF-kappaB triggers systemic TNFalpha-dependent inflammation and localized TNFalpha-independent inflammatory disease. *Genes Dev*. 2010;24: 1709–17.
- Solt LA, May MJ. The IkkappaB kinase complex: master regulator of NF-kappaB signalling. *Immunol Res*. 2008;42:3–18.
- Craggs L, Kalaria RN. Revisiting dietary antioxidants, neurodegeneration and dementia. *Neuroreport*. 2011;22:1–3.
- Boocock DJ, Patel KR, Faust GE, et al. Quantitation of trans-resveratrol and detection of its metabolites in human plasma and urine by high performance liquid chromatography. *J Chromatogr B Analyt Technol Biomed Life Sci*. 2007;848:182–7.
- Meng X, Maliakal P, Lu H, Lee MJ, Yang CS. Urinary and plasma levels of resveratrol and quercetin in humans, mice, and rats after ingestion of pure compounds and grape juice. *J Agric Food Chem*. 2004;52:935–42.
- Bishayee A, Waghray A, Barnes KF, et al. Suppression of the inflammatory cascade is implicated in resveratrol chemoprevention of experimental hepatocarcinogenesis. *Pharm Res*. 2010;27:1080–91.
- Boily G, He XH, Pearce B, Jardine K, McBurney MW. SirT1-null mice develop tumors at normal rates but are poorly protected by resveratrol. *Oncogene*. 2009;28:2882–9283.
- Pfister JA, Ma C, Morrison BE, D'Mello SR. Opposing effects of sirtuins on neuronal survival: SIRT1-mediated neuroprotection is independent of its deacetylase activity. *PLoS One*. 2008;3:e4090.
- Howitz KT, Bitterman KJ, Cohen HY, et al. Small molecule activators of sirtuins extend *Saccharomyces cerevisiae* lifespan. *Nature*. 2003;425: 191–6.
- Knutson MD, Leeuwenburgh C. Resveratrol and novel potent activators of SIRT1: effects on aging and age-related diseases. *Nutr Rev*. 2008;6:591–6.
- Anekonda TS. Resveratrol—a boon for treating Alzheimer's disease? *Brain Res Rev*. 2006;52:316–236.
- van Acker SA, Tromp MN, Haenen GR, van der Vijgh WJ, Bast A. Flavonoids as scavengers of nitric oxide radical. *Biochem Biophys Res Commun*. 1995;214:755–9.
- Laughton MJ, Evans PJ, Moroney MA, Hoult JR, Halliwell B. Inhibition of mammalian 5-lipoxygenase and cyclo-oxygenase by flavonoids and phenolic dietary additives. Relationship to antioxidant activity and to iron ion-reducing ability. *Biochem Pharmacol*. 1991;42:1673–81.
- Nakamaru Y, Vuppusetty C, Wada H, et al. A protein deacetylase SIRT1 is a negative regulator of metalloproteinase-9. *FASEB J*. 2009;23:2810–9.
- Woo JH, Lim JH, Kim YH, et al. Resveratrol inhibits phorbol myristate acetate-induced matrix metalloproteinase-9 expression by inhibiting JNK and PKC delta signal transduction. *Oncogene*. 2004;23:1845–53.
- Gao Z, Ye J. Inhibition of transcriptional activity of c-JUN by SIRT1. *Biochem Biophys Res Commun*. 2008;376:793–6.
- In: Rice-Evans C, Packer L, editors: *Flavonoids in Health and Disease* (second ed.), Marcel Dekker Inc, New York/Basel (2003).
- Walle T, Hsieh F, DeLegge MH, Oatis JE Jr, Walle UK. High absorption but very low bioavailability of oral resveratrol in humans. *Drug Metab Dispos*. 2004;32:1377–82.



46. Marier JF, Vachon P, Gritsas A, Zhang J, Moreau JP, Ducharme MP. Metabolism and disposition of resveratrol in rats: extent of absorption, glucuronidation, and enterohepatic recirculation evidenced by a linked-rat model. *J Pharmacol Exp Ther*. 2002;302:369–73.
47. Abd El-Mohsen M, Bayele H, Kuhnle G, et al. Distribution of [3H]trans-resveratrol in rat tissues following oral administration. *Br J Nutr*. 2006;96:62–70.
48. Yu C, Shin YG, Chow A, et al. Human, rat, and mouse metabolism of resveratrol. *Pharm Res*. 2002;19:1907–14.